ORIGINAL ARTICLE

Cancer Science WILEY

Individualized model for predicting COVID-19 deterioration in patients with cancer: A multicenter retrospective study

Bin Xu[1] 🄳 | Ke-Han Song[2] | Yi Yao[1] | Xiao-Rong Dong[3] | Lin-Jun Li[4] | Qun Wang[5] | Ji-Yuan Yang[6] | Wei-Dong Hu[7] 🄳 | Zhi-Bin Xie[8] | Zhi-Guo Luo[9] | Xiu-Li Luo[10] | Jing Liu[11] | Zhi-Guo Rao[12] | Hui-Bo Zhang[1] | Jie Wu[1] | Lan Li[1] | Hong-Yun Gong[1] | Qian Chu[13] | Qi-Bin Song[1] | Jie Wang[14] 🄳

[1]Cancer Center, Renmin Hospital of Wuhan University, Wuhan, China

[2]Department of Orthopaedic Surgery, Tongji Hospital, Tongji Medical College, Huazhong University of Science and Technology, Wuhan, China

[3]Department of Oncology, Union Hospital, Tongji Medical College, Huazhong University of Science and Technology, Wuhan, China

[4]Department of Oncology, Hubei Provincial Hospital of Integrated Chinese and Western Medicine, Wuhan, China

[5]Department of Oncology, The Fifth Hospital of Wuhan, Wuhan, China

[6]Department of Oncology, First Affiliated Hospital of Yangtze University, Jingzhou, China

[7]Department of Thoracic Surgery, Zhongnan Hospital of Wuhan University, Wuhan, China

[8]Department of Respiratory and Critical Care Medicine, Xiaogan Hospital Affiliated to Wuhan University of Science and Technology, Xiaogan, China

[9]Department of oncology, Taihe Hospital, Hubei University of Medicine, Shiyan, China

[10]Department of Oncology, Hubei Provincial Hospital of TCM, Wuhan, China

[11]Department of Oncology, Huanggang Central Hospital, Huanggang, China

[12]Department of Oncology, General Hospital of Central Theater Command, People's Liberation Army, Wuhan, China

[13]Department of Oncology, Tongji Hospital, Tongji Medical College, Huazhong University of Science and Technology, Wuhan, China

[14]Department of Medical Oncology, State Key Laboratory of Molecular Oncology, National Cancer Center/Cancer Hospital, Chinese Academy of Medical Sciences & Peking Union Medical College, Beijing, China

Correspondence
Qian Chu, Department of Oncology, Tongji Hospital, Tongji Medical College, Huazhong University of Science and Technology, Wuhan, China.
Email: qianchu@tjh.tjmu.edu.cn

Qibin Song, Cancer Center, Renmin Hospital of Wuhan University, Wuhan, China.
Email: qibinsong@whu.edu.cn

Jie Wang, State Key Laboratory of Molecular Oncology, Department of Medical Oncology, National Cancer Center/Cancer Hospital, Chinese Academy of Medical Sciences and Peking Union Medical College, Beijing, China.
Email: zlhuxi@163.com

Funding information
National Natural Science Foundation of China, Grant/Award Number: 81670123.

Abstract

The 2019 novel coronavirus has spread rapidly around the world. Cancer patients seem to be more susceptible to infection and disease deterioration, but the factors affecting the deterioration remain unclear. We aimed to develop an individualized model for prediction of coronavirus disease (COVID-19) deterioration in cancer patients. The clinical data of 276 cancer patients diagnosed with COVID-19 in 33 designated hospitals of Hubei, China from December 21, 2019 to March 18, 2020, were collected and randomly divided into a training and a validation cohort by a ratio of 2:1. Cox stepwise regression analysis was carried out to select prognostic factors. The prediction model was developed in the training cohort. The predictive accuracy of the model was quantified by C-index and time-dependent area under the receiver operating characteristic curve (t-AUC). Internal validation was assessed by the validation cohort. Risk stratification based on the model was carried out. Decision curve

analysis (DCA) were used to evaluate the clinical usefulness of the model. We found age, cancer type, computed tomography baseline image features (ground glass opacity and consolidation), laboratory findings (lymphocyte count, serum levels of C-reactive protein, aspartate aminotransferase, direct bilirubin, urea, and D-dimer) were significantly associated with symptomatic deterioration. The C-index of the model was 0.755 in the training cohort and 0.779 in the validation cohort. The t-AUC values were above 0.7 within 8 weeks both in the training and validation cohorts. Patients were divided into two risk groups based on the nomogram: low-risk (total points ≤ 9.98) and high-risk (total points > 9.98) group. The Kaplan-Meier deterioration-free survival of COVID-19 curves presented significant discrimination between the two risk groups in both training and validation cohorts. The model indicated good clinical applicability by DCA curves. This study presents an individualized nomogram model to individually predict the possibility of symptomatic deterioration of COVID-19 in patients with cancer.

KEYWORDS

cancer, COVID-19, deterioration, retrospective study, risk model

1 | INTRODUCTION

The 2019 novel coronavirus, named severe acute respiratory syndrome coronavirus 2 (SARS-CoV-2),[1,2] has spread rapidly around the world since it was initially isolated and identified in Wuhan, China, causing the pandemic of corona virus disease (COVID-19). By April 30, 2020, besides China, SARS-CoV-2 had been reported in 211 countries, with 3 131 014 confirmed cases of infection and more than 200 000 deaths. Increasing evidence indicates that all populations are generally susceptible to the SARS-CoV-2,[3-5] but elderly men with comorbidities are more likely to be affected, and develop severe respiratory diseases.[6-8]

Risk of worse prognosis of COVID-19 increases in patients with various preexisting conditions, especially those with cancer. Anticancer treatments or malignancy itself cause general immunosuppression in cancer patients, thus increase susceptibility to infection and disease deterioration.[9,10] As a result, COVID-19 patients with cancer suffer poorer outcomes, thus more attention should be paid to this cohort.

In the course of clinical treatment, the condition of some patients could deteriorate, but the factors affecting the deterioration remain unclear. In the present study, we tried to analyze the risk factors for symptomatic deterioration of COVID-19 patients with cancer by establishing a nomogram prognostic model in a large cohort of cancer patients, providing a better understanding of COVID-19 and management of infected cancer patients.

2 | MATERIALS AND METHODS

We retrospectively analyzed the medical records of cancer patients (359 cases) who were primarily diagnosed with COVID-19 in 33 designated hospitals of Hubei Province, China from December 21, 2019 to March 18, 2020. The variables included the demographic and clinical characteristics, initial symptoms of infection, chest computed tomography (CT) scan at initial diagnosis, comorbidities, clinical treatments, survival outcomes, and time. The Ethics Committee of the National Cancer Center approved this study, and waived informed consent due to the severity and rapid spread of COVID-19.

2.1 | Follow-up, primary endpoint, and event definition

The follow-up cut-off date was April 2, 2020. All the patients' survival data were available. The primary endpoint was deterioration-free survival of COVID-19 (C-DFS). The event was defined as the first symptomatic deterioration that occurred after the initial symptom assessment on admission. The C-DFS was defined as the period from the date of initial symptom assessment to the date of the first symptomatic deterioration or the date of death without deterioration. The symptomatic deterioration was defined as the deterioration of the disease severity, and the severity level assessment of COVID-19 symptoms included five levels: asymptomatic, mild, moderate, severe, and critical type, which were defined according to the 7th edition of the COVID-19 Diagnosis and Treatment Plan, released by the National Health Commission and National Administration of Traditional Chinese Medicine. The cases with unrecorded deterioration dates (55 cases), incomplete CT results (26 cases), missing symptom information (1 case), and elusive comorbidity information (1 case) were excluded, leaving 276 eligible cases that were formally enrolled in the present study (Figure S1).

TABLE 1 Demographic and clinical characteristics of cancer patients with COVID-19

	Overall (N = 276)	Training cohort (N = 183)	Validation cohort (N = 93)	P value*
Age (years)	63 (55, 70)	61 (54, 69)	65 (57, 72)	.058
Sex, male	139 (50.4)	91 (49.7)	48 (51.6)	.866
Smoking history	71 (25.7)	49 (26.8)	22 (23.7)	.678
Drinking history				.514
No	204 (73.9)	135 (73.8)	69 (74.2)	
Yes	54 (19.6)	38 (20.8)	16 (17.2)	
Unknown	18 (6.5)	10 (5.5)	8 (8.6)	
Initial symptoms				
Fever	203 (73.6)	130 (71.0)	73 (78.5)	.237
Cough	182 (65.9)	120 (65.6)	62 (66.7)	.963
Fatigue	138 (50.0)	92 (50.3)	46 (49.5)	1.000
Sputum	105 (38.0)	67 (36.6)	38 (40.9)	.578
Dyspnea	103 (37.3)	71 (38.8)	32 (34.4)	.561
Fever	103 (37.3)	71 (38.8)	32 (34.4)	.561
Headache	17 (6.2)	15 (8.2)	2 (2.2)	.062
Muscle ache	36 (13.0)	26 (14.2)	10 (10.8)	.538
Diarrhea	33 (12.0)	20 (10.9)	13 (14.0)	.588
Nausea	29 (10.5)	22 (12.0)	7 (7.5)	.345
Nasal congestion	6 (2.2)	2 (1.1)	4 (4.3)	.184
Nasal discharge	8 (2.9)	5 (2.7)	3 (3.2)	1.000
CT performance				
Bilateral involvement	230 (83.3)	152 (83.1)	78 (83.9)	1.000
Ground glass opacity	214 (77.5)	143 (78.1)	71 (76.3)	.853
Multicentric pattern	201 (72.8)	128 (69.9)	73 (78.5)	.153
Interstitial thickening	113 (40.9)	79 (43.2)	34 (36.6)	.354
Reticular pattern	68 (24.6)	41 (22.4)	27 (29.0)	.289
Consolidation	66 (23.9)	42 (23.0)	24 (25.8)	.707
Unilateral involvement	37 (13.4)	25 (13.7)	12 (12.9)	1.000
Crazy paving appearance	34 (12.3)	22 (12.0)	12 (12.9)	.987
Localized pattern	29 (10.5)	21 (11.5)	8 (8.6)	.538
Bronchiectasis	19 (6.9)	16 (8.7)	3 (3.2)	.129
Cancer type				.299
Gastrointestinal	53 (19.2)	35 (19.1)	18 (19.4)	
Lung	50 (18.1)	37 (20.2)	13 (14.0)	
Breast	36 (13.0)	21 (11.5)	15 (16.1)	
Thyroid	23 (8.3)	17 (9.3)	6 (6.5)	
Urological	21 (7.6)	11 (6.0)	10 (10.8)	
Hepatobiliary	11 (4.0)	7 (3.8)	4 (4.3)	
Leukemia	11 (4.0)	9 (4.9)	2 (2.2)	
Lymphoma	12 (4.3)	8 (4.4)	4 (4.3)	
Esophageal	9 (3.3)	3 (1.6)	6 (6.5)	
Other	50 (18.1)	35 (19.1)	15 (16.1)	
Comorbidities				
Hypertension	93 (33.7)	56 (30.6)	37 (39.8)	.164
Diabetes	40 (14.5)	20 (10.9)	20 (21.5)	.029

(Continues)

TABLE 1 (Continued)

	Overall (N = 276)	Training cohort (N = 183)	Validation cohort (N = 93)	P value*
Cerebrovascular	16 (5.8)	10 (5.5)	6 (6.5)	.953
COPD	17 (6.2)	13 (7.1)	4 (4.3)	.436
Chronic liver disease	19 (6.9)	15 (8.2)	4 (4.3)	.316
Chronic renal disease	12 (4.3)	6 (3.3)	6 (6.5)	.363
Comorbidity number	1 (0, 1)	0 (0, 1)	1 (0, 1)	.025
Cancer treatment within 2 months before COVID-19				.955
No/unknown	149 (54.0)	102 (55.7)	47 (50.5)	
Chemotherapy	31 (11.2)	20 (10.9)	11 (11.8)	
Radiotherapy	7 (2.5)	4 (2.2)	3 (3.2)	
Surgery	21 (7.6)	14 (7.7)	7 (7.5)	
Targeted	14 (5.1)	10 (5.5)	4 (4.3)	
Combination	14 (5.1)	8 (4.4)	6 (6.5)	
Other/unknown	40 (14.5)	25 (13.7)	15 (16.1)	
Laboratory findings				
WBC (10^9/L)	5.21 (3.81, 6.73)	4.78 (3.68, 6.40)	5.28 (3.96, 6.85)	.274
Neutrophils (10^9/L)	3.54 (2.57, 5.11)	3.19 (2.55, 4.58)	3.64 (2.60, 5.25)	.287
LYM (10^9/L)	0.82 (0.55, 1.26)	0.91 (0.58, 1.32)	0.78 (0.54, 1.24)	0.310
MONO (10^9/L)	0.40 (0.27, 0.59)	0.40 (0.23, 0.54)	0.41 (0.29, 0.60)	.299
EO (10^9/L)	0.03 (0.00, 0.09)	0.03 (0.01, 0.09)	0.04 (0.00, 0.09)	.770
BASO (10^9/L)	0.01 (0.01, 0.02)	0.01 (0.00, 0.02)	0.01 (0.01, 0.02)	.357
PLT (10^9/L)	191.00 (125.75, 246.00)	174.00 (117.00, 222.60)	197.00 (139.00, 252.00)	.080
CRP (mg/L)	28.20 (10.86, 71.16)	33.04 (11.24, 58.57)	26.80 (9.87, 74.89)	.976
ALT (U/L)	21.50 (13.00, 36.00)	22.00 (12.00, 33.00)	21.00 (14.00, 38.45)	0.432
AST (U/L)	27.00 (19.00, 39.00)	27.00 (18.00, 37.00)	27.00 (19.00, 39.00)	.883
TBIL (μmol/L)	10.32 (7.50, 14.25)	10.10 (8.00, 13.50)	10.70 (7.35, 14.55)	.759
DBIL (μmol/L)	3.60 (2.40, 5.20)	3.60 (2.40, 5.20)	3.70 (2.40, 5.20)	.680
Urea (mmol/L)	4.80 (3.50, 6.75)	4.91 (3.31, 7.52)	4.70 (3.63, 6.52)	.682
CRE (μmol/L)	64.55 (52.22, 81.05)	63.00 (52.90, 82.80)	65.00 (52.15, 79.90)	.879
PCT (ng/ml)	0.11 (0.05, 0.24)	0.10 (0.05, 0.26)	0.12 (0.05, 0.22)	.989
PT (s)	12.80 (11.70, 13.70)	12.60 (11.60, 13.50)	12.90 (11.80, 13.70)	.370
APTT (s)	32.69 (28.48, 38.08)	32.72 (28.60, 38.30)	32.50 (28.30, 37.90)	.950
D2 (mg/L)	0.86 (0.40, 1.95)	0.79 (0.40, 1.44)	0.96 (0.41, 2.12)	.450

Note: Data are shown as n (%) or median (interquartile range).

Abbreviations: ALT, alanine aminotransferase; APTT, activated partial thromboplastin time; AST, aspartate aminotransferase; BASO, basophils; COPD, chronic obstructive pulmonary disease; CRE, creatinine; CRP, C-reactive protein; CT, computed tomography; D2, D-dimer; DBIL, direct bilirubin; EO, eosinophil; LYM, lymphocytes; MONO, monocytes; PCT, procalcitonin; PLT, platelets; PT, prothrombin time; TBIL, total bilirubin; WBC, white blood cells.

*P value is derived from the Wilcoxon test (for continuous variables) and Chi-square test/Fisher exact test (for categorized variables) between training and validation cohort.

2.2 | Statistical analysis

Patient data were randomly assigned to the training cohort and the validation cohort by a ratio of 2:1. The Kaplan-Meier method was applied to estimate C-DFS. In the training cohort, we used the least absolute shrinkage and selection operator (LASSO) regression analysis[11] to select the characteristic variables of CT scans and clinical symptoms that might have potential clinical significance to influence C-DFS, then the symptom LASSO score and CT LASSO score were built according to the following formula. The cut-off point of symptom and CT LASSO score was selected based on log-rank statistics:

$$\text{LASSO score} = \sum_{i}^{n} i * \text{coefficient (i)} \, ; \text{for i in predictors}$$

Cox univariate regression analysis and Cox stepwise regression based on the Akaike information criterion minimum principle were then carried out to select prognostic factors. The predictive accuracy of the regression model was quantified by the C-index. The C-index value varies from 0.5, which indicates a completely random chance, to 1.0, which indicates a perfect fit. Typically, a C-index value above 0.7 suggests a reasonable model.

The calibration plot was used to compare actual and predicted probabilities of 2-week, 4-week, and 8-week C-DFS rates from the model. In the calibration plot, the closer the solid line is to the dashed line, the more accurately the model performs to predict C-DFS. We then verified the reliability of the nomogram model by means of the area under receiver operating characteristic curves (AUC) value at different time points, namely time-dependent AUC (t-AUC). A t-AUC value above 0.7 suggests that a stable and continuous prediction model has been constructed. Decision curve analysis (DCA)[12,13] was used to evaluate the clinical usefulness of the model.

Finally, log-rank statistics were applied to create a risk stratification according to the total risk scores based on the nomogram to illustrate the independent discrimination ability of the nomogram model. All analyses were undertaken in R software (version 3.6.1). A value of $P < .05$ was statistically significant for all analyses.

3 | RESULTS

3.1 | Characteristics of patients and disease

A total of 276 patients were enrolled in the present study and assigned into the training cohort (n = 183) and the validation cohort (n = 93). The median follow-up time was 43 days in the whole patient group, 42 days in the training cohort, and 43 days in the validation cohort. Median C-DFS was not reached in either cohort (Figure S2). The demographic and clinical characteristics of cancer patients with COVID-19 are summarized in Table 1. The median age of the patients was 63 (interquartile range [IQR], 55-70) in the whole population, 61 (IQR, 51-69) years in the training cohort, and 65 (IQR, 57-72) years in the validation cohort, respectively. For the overall population, the training cohort, and the validation cohort, the most common initial symptoms were fever (73.6%, 71.0%, and 78.5%), cough (65.9%, 65.6%, and 66.7%), fatigue (50.0%, 50.3%, and 49.5%); the most common baseline CT image features were bilateral involvement (83.3%, 83.1%, and 83.9%), ground glass opacity (77.5%, 78.1%, and 76.3%), and multicentric pattern (72.8%, 69.9%, and 78.5%), respectively. Among all patients, those with gastrointestinal cancer, lung cancer, and breast cancer constituted the majority of the enrolled population. The most common comorbidities were hypertension and diabetes. One hundred and forty-nine (54.0%) patients did not receive cancer treatment within the 2 months before COVID-19. Specific treatment approaches and laboratory findings are listed in Table 1.

3.2 | Least absolute shrinkage and selection operator for variable selection and score building

Among all the 12 analyzed symptom features, two features (dyspnea and fatigue) were considered to be potentially predictive (referred to hereafter as predictors) on the basis of patients in the training cohort (Figure 1A,B) using the LASSO Cox regression analysis, which were further used to build a symptom LASSO score (coefficient: dyspnea 0.231, fatigue 0.043). The same analyzing process was applied for CT performance, where two of 10 CT image features (ground glass opacity and consolidation) were considered as predictors (Figure 1C,D), and CT LASSO score was calculated (coefficient: ground glass opacity −0.006, consolidation 0.632). Six of 18 laboratory findings (lymphocyte count [LYM], serum levels of C-reactive protein [CRP], aspartate aminotransferase [AST], direct bilirubin [DBIL], urea, and D-dimer [D2]) were selected as predictors (Figure 1E,F), and laboratory LASSO score was calculated (coefficient: LYM −0.135, CRP 0.004, AST 5.597, DBIL 0.011, urea 0.003, D2 0.031).

3.3 | Variable selection for construction of individual prognostic model

According to the Cox univariate regression analysis, age, cancer types, CT LASSO score, symptoms LASSO score, and laboratory LASSO score could predict worse C-DFS in COVID-19 patients with cancer. Finally, age, cancer type, symptoms LASSO score, CT LASSO score, and laboratory LASSO score were incorporated into the model according to multivariate regression analysis. The results of the Cox multivariate analysis for selected variables are shown in Table 2.

3.4 | Development and validation of the individualized prediction model

A nomogram based on the model that incorporated the selected variables was established (Figure 2A). The total points were determined based on the score of each variable that was calculated. The predictive ability of the nomogram for individual deterioration risk possibility was then evaluated in the training cohort and independently validated in the validation cohort.

The C-index of the nomogram was 0.755 in the training cohort and 0.779 in the validation cohort. Figure 2B shows that t-AUC values were above 0.7 for the prediction of deterioration risk within 8 weeks both in the training and validation cohort, indicating that a stable and continuous prediction model was successfully constructed.

Furthermore, the calibration curves of the nomogram showed high consistencies between the predicted and observed 2-week, 4-week, and 8-week C-DFS probability both in the training and validation cohorts (Figure 2C-H). In summary, the nomogram showed considerable discriminative and calibrating abilities.
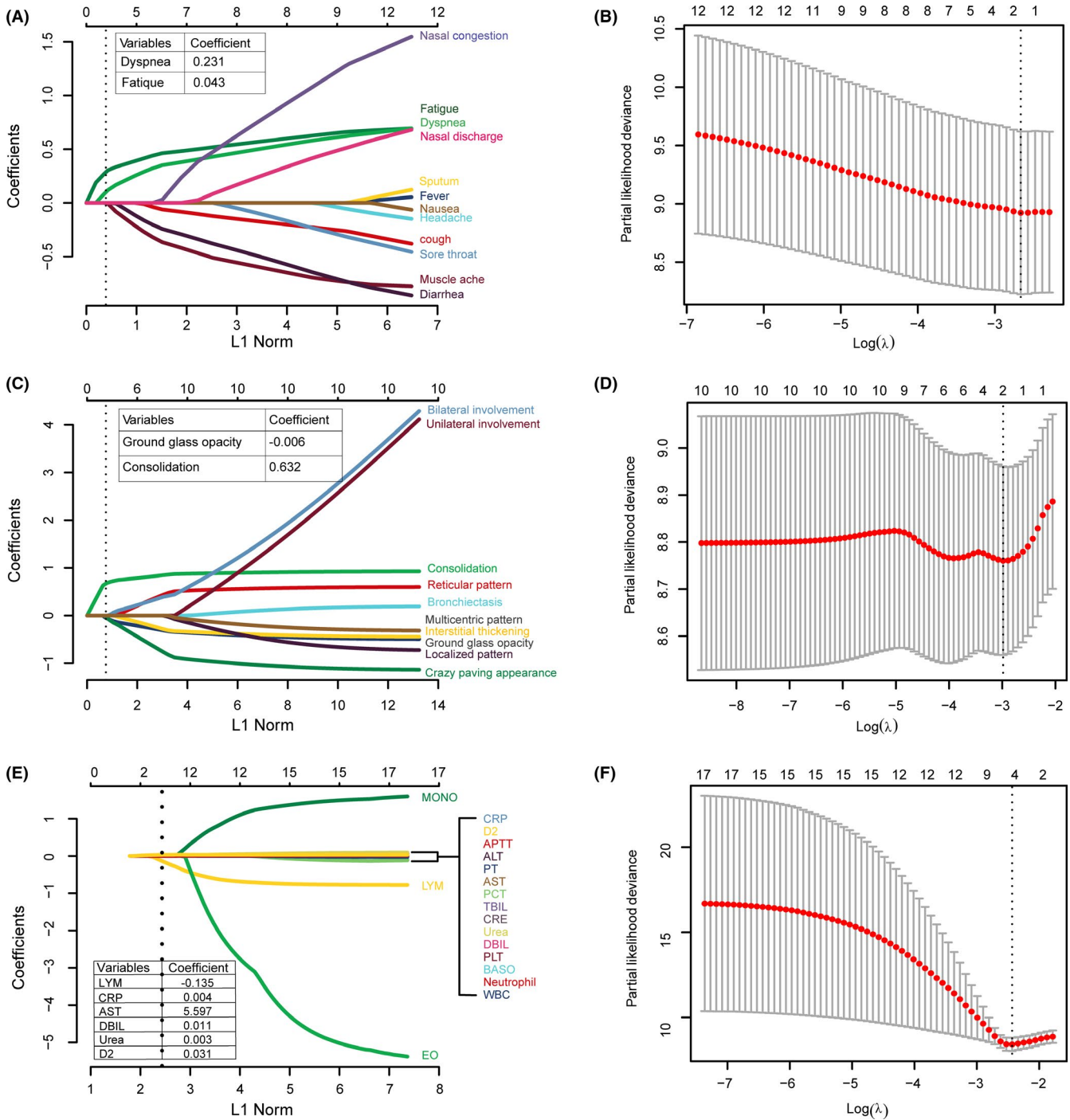
FIGURE 1 Predictor selection based on least absolute shrinkage and selection operator (LASSO) regression analysis of COVID-19 deterioration in patients with cancer. A, LASSO coefficient profiles of the 12 symptoms. A coefficient profile plot was produced against the λ sequence. Vertical line was drawn at the value selected using 10-fold cross-validation, where optimal λ (0.070) resulted in two nonzero coefficients. B, λ selection in the LASSO analysis used 10-fold cross-validation by minimum criteria for 12 symptoms. The partial likelihood deviance was plotted against λ. Dotted vertical lines were drawn at the optimal values (0.070) by using the minimum criteria. C, LASSO coefficient profiles of the 10 computed tomography (CT) image features. A coefficient profile plot was produced against the λ sequence. Vertical line was drawn at the value selected using 10-fold cross-validation, where optimal λ (0.051) resulted in two nonzero coefficients. D, λ selection in the LASSO analysis used 10-fold cross-validation by minimum criteria for 10 CT image features. The partial likelihood deviance was plotted against λ. Dotted vertical lines were drawn at the optimal values (0.051) by using the minimum criteria. E, LASSO coefficient profiles of 18 laboratory findings. A coefficient profile plot was produced against the λ sequence. Dotted vertical lines were drawn at the optimal values (0.088) by using the minimum criteria. F, λ selection in the LASSO analysis used 10-fold cross-validation by minimum criteria for 18 laboratory findings. The partial likelihood deviance was plotted against λ. Dotted vertical lines were drawn at the optimal values (0.088) by using the minimum criteria

TABLE 2 Univariate and multivariate Cox analyses for predicting deterioration-free survival of COVID-19 C-DFS in the training cohort of cancer patients

	Univariate analysis			Multivariate analysis[a]		
	HR	95% CI	*P* value	HR	95% CI	*P* value
Age (years)						
<75	Ref	-	-	Ref	-	-
≥ 75	1.955	1.018-3.751	**.044**	2.305	1.093-4.864	**.0280**
Gender						
Female	Ref	-	-	-	-	-
Male	1.440	0.818-2.537	.206	-	-	-
Smoking history						
No	Ref	-	-	-	-	-
Yes	1.541	0.856-2.777	.150	-	-	-
Drinking history						
No	Ref	-	-	-	-	-
Yes	0.999	0.494-2.018	.997	-	-	-
Unknown	1.804	0.639-5.094	.265	-	-	-
Cancer type						
Breast	Ref	-	-	Ref	-	1.0000
Esophageal	8.780	1.233-62.526	.030	4.319	0.543-34.353	.1667
Gastrointestinal	1.867	0.377-9.252	.445	1.141	0.223- 5.833	.8743
Hepatobiliary	3.825	0.537-27.255	.181	2.826	0.381-20.962	.3095
Leukemia	5.485	1.004-29.975	**.050**	3.025	0.532-17.193	.2117
Lung	4.129	0.924-18.457	.063	4.602	1.017-20.832	**.0475**
Lymphoma	12.263	2.358-63.766	**.003**	9.619	1.799-51.435	**.0081**
Thyroid	1.881	0.314-11.274	.489	3.170	0.509-19.735	.2163
Urological	7.996	1.659-38.530	**.010**	1.978	0.371-10.561	.4248
Other	1.881	0.380-9.325	.439	2.229	0.443-11.205	.3307
Cancer treatment before COVID-19[a]						
No	Ref	-	-	-	-	-
Chemotherapy	1.533	0.621-3.785	.354	-	-	-
Radiotherapy	1.455	0.196-10.815	.714	-	-	-
Surgery	2.174	0.880-5.368	.092	-	-	-
Targeted	1.459	0.436-4.884	.540	-	-	-
Combination	2.671	0.919-7.764	.071	-	-	-
Other	1.317	0.562-3.087	.526	-	-	-
Diabetes	0.718	0.258-1.996	.525	-	-	-
Hypertension	1.166	0.641-2.119	.615	-	-	-
Cerebrovascular disease	1.102	0.343-3.545	.870	-	-	-
COPD	1.712	0.728-4.022	.218	-	-	-
Chronic liver disease	0.475	0.115-1.958	.303	-	-	-
Chronic renal disease	2.071	0.644-6.662	.222	-	-	-
Symptom LASSO score						
≤0.231	Ref	-	-	Ref	-	-
>0.231	2.221	1.250-3.948	**.007**	1.463	0.765-2.797	.2510
CT LASSO score						
≤0	Ref	-	-	Ref	-	-
>0	2.686	1.518-4.752	**.001**	2.145	1.057-4.354	**.0350**

(Continues)

TABLE 2 (Continued)

	Univariate analysis			Multivariate analysis[a]		
	HR	95% CI	P value	HR	95% CI	P value
Laboratory LASSO score						
≤0.498	Ref	-	-	Ref	-	-
>0.498	5.043	2.871-8.858	**<.001**	4.158	2.087-8.283	**<.0010**

Note: Bold values indicate significance.

Abbreviations: -, not included in analysis; CI, confidence interval; COPD, chronic obstructive pulmonary disease; CT, computed tomography; HR, hazard ratio; LASSO, least absolute shrinkage and selection operator; Ref, reference.

[a]Antitumor therapies used more than 2 months prior to COVID-19 infection were not included.
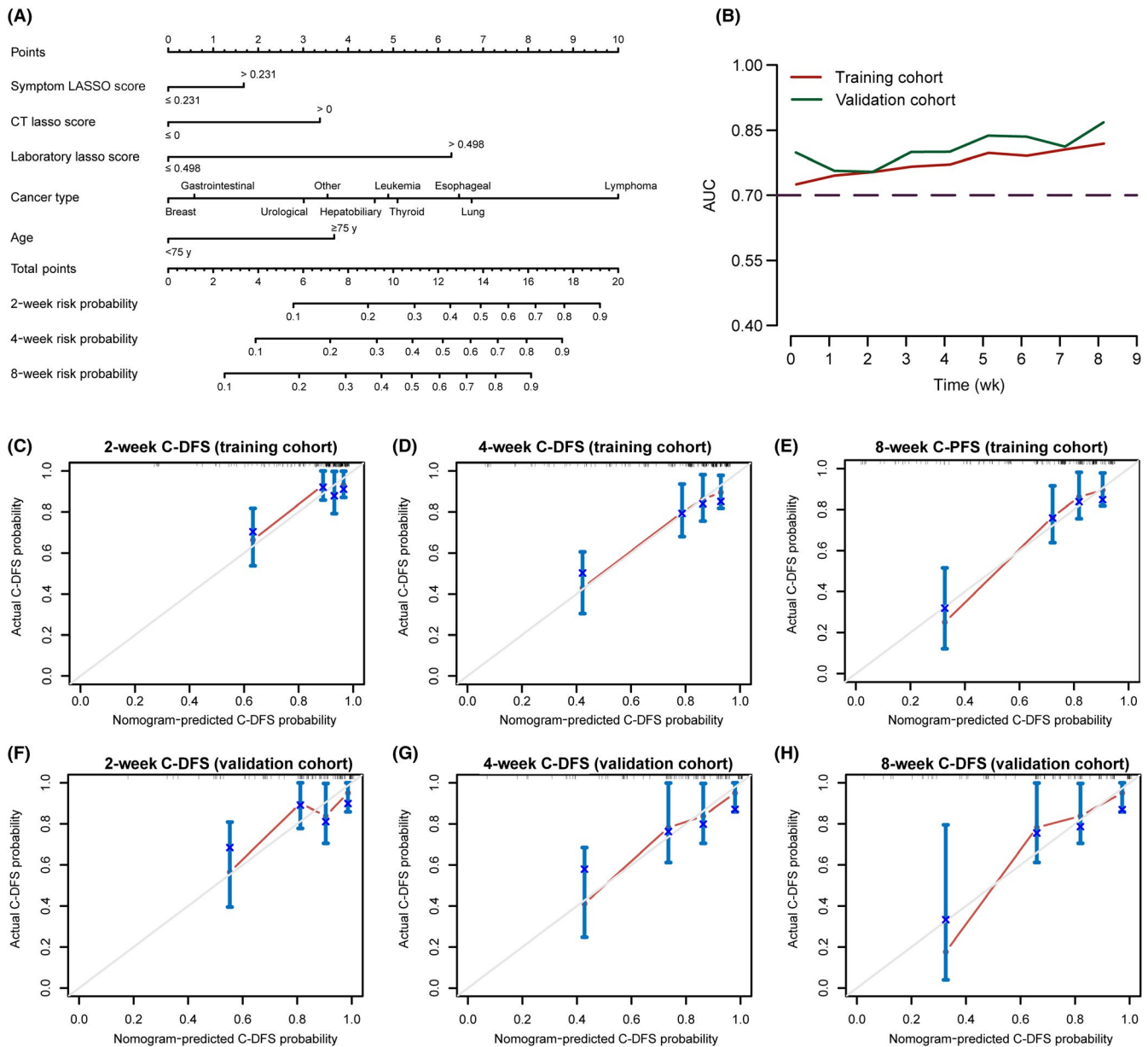
FIGURE 2 Nomogram model construction and calibration curves for validation. A, Nomogram constructed for risk prediction of symptomatic deterioration of cancer patients with COVID-19. B, Time-dependent area under the receiver operating characteristic curve (AUC) of the nomogram model in the training cohort and validation cohort. C-E, Calibration curves of the 2-, 4-, and 8-week deterioration-free survival of COVID-19 (C-DFS) for patients in the training cohort. F-H, Calibration curves of the 2-, 4-, and 8-week C-DFS for patients in the validation cohort. Gray line indicates the ideal reference line where predicted probabilities would match the observed survival rates. Red dots are calculated by bootstrapping (resample: 1000) and represent the performance of the nomogram. The closer the solid red line is to the gray line, the more accurately the model predicts survival. LASSO, least absolute shrinkage and selection operator

3.5 | Clinical applications

Decision curve analysis was carried out to evaluate the clinical usefulness of the nomogram by quantifying the net benefits at different threshold probabilities (Figure 3). It showed more net benefits across a wider range of threshold probabilities than either the treat-all-patients scheme or the treat-none scheme both in the training cohort and validation cohort.

3.6 | Risk stratification based on the nomogram

Finally, a risk stratification was made based on the nomogram. Coronavirus disease patients with cancer were assigned into two risk groups according to their total points: low-risk (total points of 9.98 or less) group and high-risk (total points more than 9.98) group based on standardized log-rank statistics (Figure 4A). The risk plot showed that the progressed events occurred more frequently in high-risk group in both the training and validation cohort (Figure 4B,C).

The Kaplan-Meier C-DFS curves (Figure 4D,E) presented the significant discrimination among the two risk groups both in the training (log-rank $P < .001$) and the validation cohort (log-rank $P = .016$). Hazard ratio (HR) values of the high-risk group vs low-risk group were 6.755 (95% confidence interval [CI], 3.804-12.000; $P < .001$) in the training cohort and 2.629 (95% CI, 1.166-5.927; $P = .016$) in the validation cohort. Furthermore, propensity score matching (PSM) was applied, where the two risk groups were matched by 1:1 to balance the potential between-group bias (Tables S1 and S2). The results showed that HR values of the high-risk group vs low-risk group after PSM were 2.135 (95% CI, 1.144-3.986, $P = .013$) in the training cohort and 4.943 (95% CI, 1.066-22.930, $P = .024$) in the validation cohort. The Kaplan-Meier C-DFS curves (Figure 4E,F) still showed significant difference between the two risk groups in the training cohort and the validation cohort.

4 | DISCUSSION

The establishment of clinical prognostic models is of great importance for predicting the outcome of disease and guiding clinical decisions. A nomogram uses clinical, pathological, or other features to establish a statistical predictive model that can provide the possibility of a certain clinical event.[13-15]

In this pioneering study, we incorporated age, clinical symptoms, CT image features, cancer types, and laboratory findings to develop a nomogram model for individually predicting symptomatic deterioration in COVID-19 patients with cancers as a preexisting condition. The nomogram model was validated by a variety of statistical methods and proved to be accurate. The C-indexes of our nomogram were 0.755 in the training cohort and 0.779 in the validation cohort, and the calibration curves were highly consistent among the predicted and observed 2-week, 4-week, and 8-week C-DFS probabilities, indicating that a stable prediction model was constructed. More importantly, the model indicated good clinical applicability by DCA curves.

In the course of clinical treatment, the symptoms of some patients could worsen. This is the first study to undertake risk stratification targeting high-risk cancer patients for COVID-19 symptomatic deterioration based on the nomogram, thus helping clinicians to make more informed decisions to treat patients at the possibly earliest time before life-threatening symptoms occur. We found that age, cancer type (lung cancer and lymphoma), CT image features (ground glass opacity and consolidation) and laboratory findings (LYM, CRP, AST, DBIL, urea, and D2) are risk factors of symptomatic deterioration (Table 2).

A recent study from Liang et al[9] found that COVID-19 patients with cancer had a higher risk of severe events compared with patients without cancer (7 of 18 [39%] patients vs 124 of 1572 [8%] patients, $P = .0003$). Another study from Zhang et al[16] also showed that a high proportion (15 of 28 [53.6%]) of patients had severe events
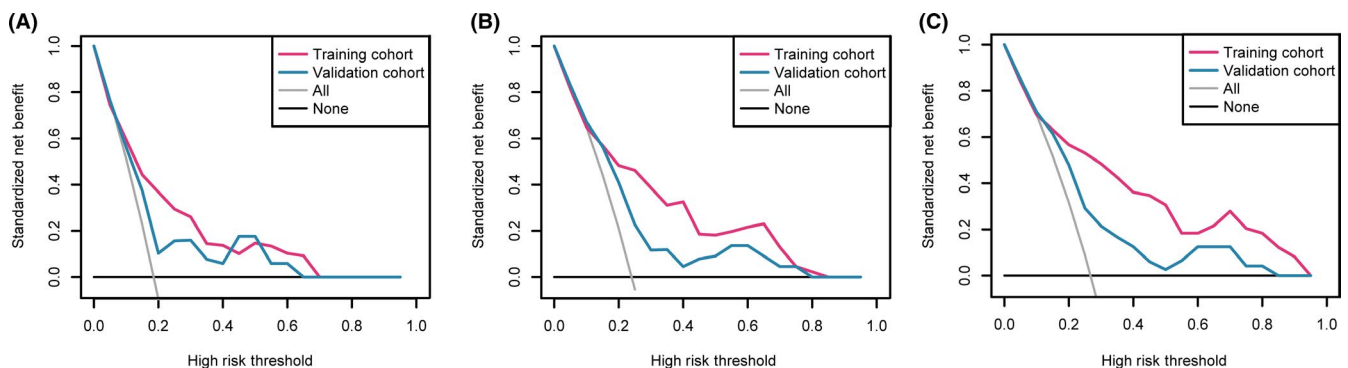

FIGURE 3 Decision curve analysis of 2-, 4- and 8-week deterioration-free survival of COVID-19 in cancer patients. Gray lines represent the assumption that all patients have symptomatic deterioration. Black lines represent the hypothesis that no patients have symptomatic deterioration. The *Y*-axis measures the net benefit. The net benefit was calculated by subtracting the proportion of all patients who are false deterioration from the proportion who are true deterioration, and then weighting the relative harm of abandoning treatment against the negative consequences of unnecessary treatment. The *X*-axis represents threshold probability (Pt). When a patient's probability of symptom deterioration (Pi) is greater than the Pt, we define it as a positive event and require clinical intervention
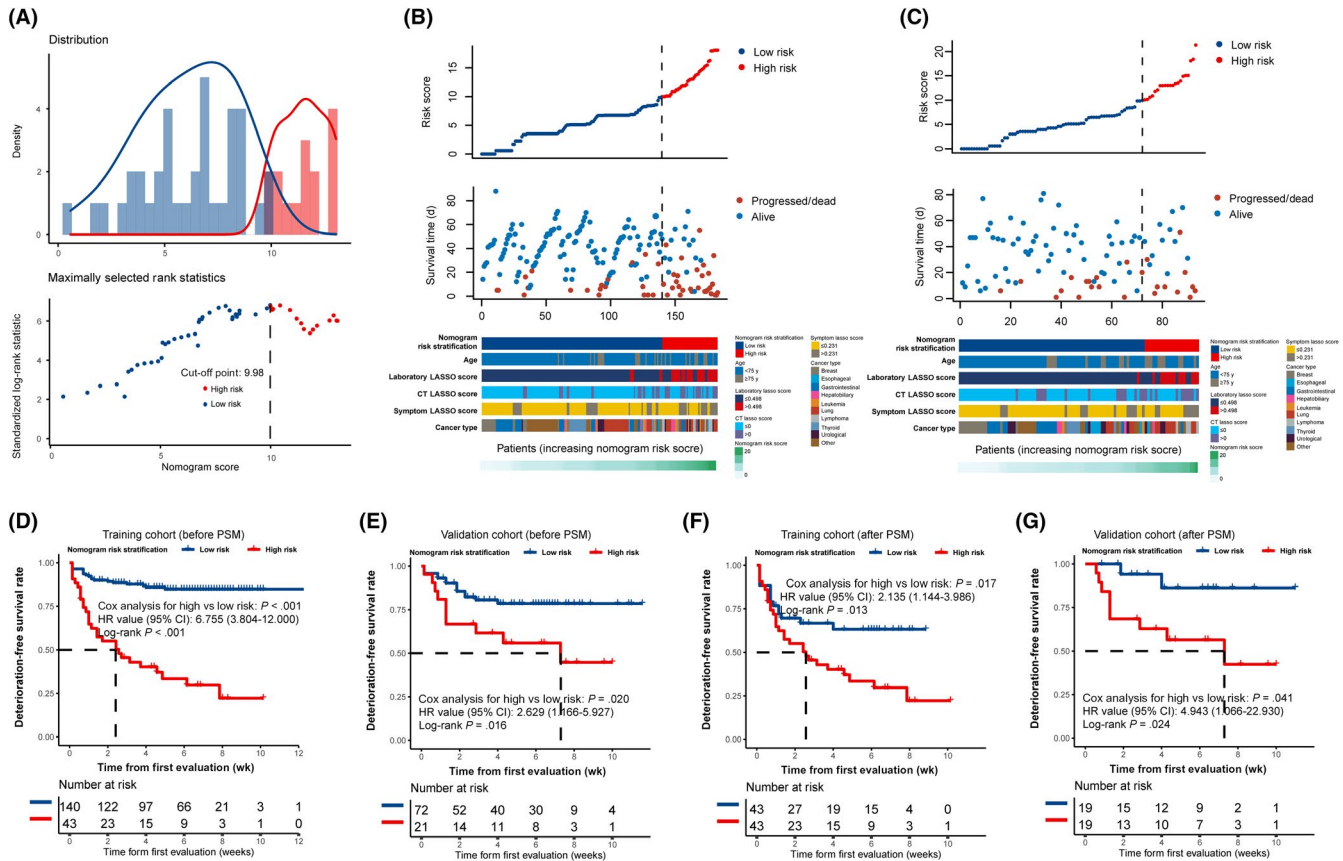
FIGURE 4 Analyses for cancer patients at different risks stratified by the nomogram. A, Cut-off point selection for risk stratification according to nomogram scores. The dotted line is drawn at the value selected based on standardized log-rank statistics. B, C, Risk plots to show the distribution pattern of nomogram scores, event and nomogram variables in training and validation cohorts. The samples were ranked by increasing nomogram scores. Dotted lines are drawn at the cut-off point selected. D, E, Kaplan-Meier curves of deterioration-free survival of COVID-19 (C-DFS) at different risks in the training and validation cohorts (before propensity score matching [PSM]). F, G, Kaplan-Meier curves of C-DFS at different risks in the training and validation cohorts (after PSM). CI, confidence interval; CT, computed tomography; HR, hazard ratio; LASSO, least absolute shrinkage and selection operator

and the mortality rate was 28.6%. The risk significantly increased (HR 4.079) if patients received antitumor treatment within 14 days before being diagnosed with COVID-19. However, the sample sizes of these early studies were too small to provide sufficient statistical power to a definite conclusion.

In our study, for the first time, we found that cancer type was a critical factor that affected symptomatic deterioration in COVID-19 patients. In the nomogram, COVID-19 patients with lymphoma had the highest risk score for symptomatic deterioration. The specific risk scores of different cancer types can be seen in the nomogram in Figure 2. Patients with COVID-19 and clinical symptoms such as dyspnea and fatigue had higher risks for symptomatic deterioration. In addition, we found that consolidation on CT was associated with a higher risk of deterioration, which was consistent with the findings in the study from Zhang et al.[16] Age was also an important risk factor for symptom progression in COVID-19 patients with cancer, which was consistent with other studies.[17-19]

To conclude, in the COVID-19 pandemic, our nomogram provides personalized prediction of the probability of symptomatic deterioration in COVID-19 patients with cancer. We strongly recommend its use in COVID-19 patients with cancer, and hopefully this powerful tool/method will help clinicians all over the world take more comprehensive and timely measures to prevent symptomatic deterioration and reduce mortality.

to Wuhan University of Science and Technology, Wuhan Fourth Hospital, Tongji Medical College, Huazhong University of Science and Technology, The Central Hospital of Wuhan, Tongji Medical College, Huazhong University of Science and Technology, Ezhou Central Hospital, The First People's Hospital of Guangshui, Affiliated Dongfeng Hospital, Hubei University of Medicine, Gong'an County People's Hospital, Hubei No. 3 People's Hospital, Jingzhou Central Hospital, The Central Hospital of Enshi Tujia and Miao Autonomous Prefecture, Xiangyang No. 1 People's Hospital, and Hubei University of Medicine) for providing patient data and their strong support for our research. We thank all authors for their efforts in collecting patient data. Finally, we thank all patients involved in the study. The study was supported by National Natural Science Foundation of China (Grant No. 81670123).

DISCLOSURE

The authors have no conflict of interest.

ORCID

Bin Xu 🆔 https://orcid.org/0000-0002-0499-0430

Wei-Dong Hu 🆔 https://orcid.org/0000-0003-3646-8572

Jie Wang 🆔 https://orcid.org/0000-0002-5602-0487

REFERENCES

1. McCloskey B, Zumla A, Ippolito G, et al. Mass gathering events and reducing further global spread of COVID-19: a political and public health dilemma. *Lancet.* 2020;395(10230):1096-1099. https://doi.org/10.1016/S0140-6736(20)30681-4

2. Li G, De Clercq E. Therapeutic options for the 2019 novel coronavirus (2019-nCoV). *Nat Rev Drug Discov.* 2020;19(3):149-150. https://doi.org/10.1038/d41573-020-00016-0

3. Habibzadeh P, Stoneman EK. The novel coronavirus: A bird's eye view. *Int J Occup Environ Med.* 2020;11(2):65-71. https://doi.org/10.15171/ijoem.2020.1921

4. Li JY, You Z, Wang Q, et al. The epidemic of 2019-novel-coronavirus (2019-nCoV) pneumonia and insights for emerging infectious diseases in the future. *Microbes Infect.* 2020;22(2):80-85. https://doi.org/10.1016/j.micinf.2020.02.002

5. Tu H, Tu S, Gao S, Shao A, Sheng J. The epidemiological and clinical features of COVID-19 and lessons from this global infectious public health event. *J Infect.* 2020;81:1-9. https://doi.org/10.1016/j.jinf.2020.04.011

6. Chen N, Zhou M, Dong X, et al. Epidemiological and clinical characteristics of 99 cases of 2019 novel coronavirus pneumonia in Wuhan, China: a descriptive study. *Lancet.* 2020;395(10223):507-513. https://doi.org/10.1016/S0140-6736(20)30211-7

7. Huang C, Wang Y, Li X, et al. Clinical features of patients infected with 2019 novel coronavirus in Wuhan, China. *Lancet.* 2020;395(10223):497-506. https://doi.org/10.1016/S0140-6736(20)30183-5

8. Xu X-W, Wu X-X, Jiang X-G, et al. Clinical findings in a group of patients infected with the 2019 novel coronavirus (SARS-Cov-2) outside of Wuhan, China: retrospective case series. *BMJ.* 2020;368:m606. https://doi.org/10.1136/bmj.m606

9. Liang W, Guan W, Chen R, et al. Cancer patients in SARS-CoV-2 infection: a nationwide analysis in China. *Lancet Oncol.* 2020;21(3):335-337. https://doi.org/10.1016/S1470-2045(20)30096-6

10. Yu J, Ouyang W, Chua MLK, Xie C. SARS-CoV-2 Transmission in patients with cancer at a tertiary care hospital in Wuhan, China. *JAMA Oncol.* 2020;25:e200980. https://doi.org/10.1001/jamaoncol.2020.0980

11. Sauerbrei W, Royston P, Binder H. Selection of important variables and determination of functional form for continuous predictors in multivariable model building. *Stat Med.* 2007;26(30):5512-5528. https://doi.org/10.1002/sim.3148

12. Vickers AJ, Cronin AM, Elkin EB, Gonen M. Extensions to decision curve analysis, a novel method for evaluating diagnostic tests, prediction models and molecular markers. *BMC Med Inf Decis Mak.* 2008;8(1):53. https://doi.org/10.1186/1472-6947-8-53

13. Huang YQ, Liang CH, He L, et al. Development and validation of a radiomics nomogram for preoperative prediction of lymph node metastasis in colorectal cancer. *J Clin Oncol.* 2016;34(18):2157-2164. https://doi.org/10.1200/JCO.2015.65.9128

14. Iasonos A, Schrag D, Raj GV, Panageas KS. How to build and interpret a nomogram for cancer prognosis. *J Clin Oncol.* 2008;26(8):1364-1370. https://doi.org/10.1200/JCO.2007.12.9791

15. Maurichi A, Miceli R, Eriksson H, et al. Factors affecting sentinel node metastasis in Thin (T1) cutaneous melanomas: development and external validation of a predictive nomogram. *J Clin Oncol.* 2020;38(14):1591-1601. https://doi.org/10.1200/JCO.19.01902

16. Zhang L, Zhu F, Xie L, et al. Clinical characteristics of COVID-19-infected cancer patients: a retrospective case study in three hospitals within Wuhan, China. *Ann Oncol.* 2020;31(7):894-901. https://doi.org/10.1016/j.annonc.2020.03.296

17. Wang H, Zhang L. Risk of COVID-19 for patients with cancer. *Lancet Oncol.* 2020;21(4):e180. https://doi.org/10.1016/S1470-2045(20)30150-9

18. Mourey L, Falandry C, de Decker L, et al. Taking care of older patients with cancer in the context of COVID-19 pandemic. *Lancet Oncol.* 2020;21(5):e236. https://doi.org/10.1016/S1470-2045(20)30229-1

19. Wang D, Hu B, Hu C, et al. Clinical characteristics of 138 hospitalized patients with 2019 novel coronavirus-infected pneumonia in Wuhan, China. *JAMA.* 2020;323(11):1061-1069. https://doi.org/10.1001/jama.2020.1585

SUPPORTING INFORMATION

Additional supporting information may be found online in the Supporting Information section.